



USDOT Region V Regional University Transportation Center Final Report

NEXTRANS Project No. 049IY02

Effect of Friction on Rolling Tire – Pavement Interaction

By

Hao Wang

Department of Civil and Environmental Engineering
University of Illinois at Urbana-Champaign
haowang4@illinois.edu

and

Imad L. Al-Qadi

Founder Professor of Engineering
Illinois Center for Transportation, Director
Department of Civil and Environmental Engineering
University of Illinois at Urbana-Champaign
alqadi@illinois.edu

and

Ilinca Stanciulescu

Assistant Professor

Department of Civil and Environmental Engineering
Rice University
ilinc@rice.edu



DISCLAIMER

Funding for this research was provided by the NEXTRANS Center, Purdue University under Grant No. DTRT07-G-005 of the U.S. Department of Transportation, Research and Innovative Technology Administration (RITA), University Transportation Centers Program. The contents of this report reflect the views of the authors, who are responsible for the facts and the accuracy of the information presented herein. This document is disseminated under the sponsorship of the Department of Transportation, University Transportation Centers Program, in the interest of information exchange. The U.S. Government assumes no liability for the contents or use thereof.



USDOT Region V Regional University Transportation Center Final Report

TECHNICAL SUMMARY

NEXTRANS Project No. 0491Y02

Final Report, November 2010

Effect of Friction on Rolling Tire – Pavement Interaction

Introduction

Accurate modeling of tire-pavement contact behavior (i.e., distribution of contact tractions at the interface) plays an important role in the analysis of pavement performance and vehicle driving safety. The tire-pavement contact is essentially a rolling contact problem. Many aspects, such as the transient contact with nonlinear frictional properties at the tire-pavement interface, make the rolling contact problem more difficult than it may appear at first glance. The nonlinear frictional contact could introduce numerical difficulties into the finite element method (FEM) solution because the contact area and distribution of the contact tractions are not known beforehand. Therefore, it is appealing to formulate and implement high-fidelity FE models capable of accurately simulating the tire-pavement contact behavior. However, obtaining an accurate frictional relationship is difficult for tire-pavement interaction. The friction between the tire and pavement is a complex phenomenon depending on many factors, such as viscoelastic properties of rubber, pavement texture, temperature, vehicle speed, slip ratio, and normal pressure. Field measurements have clearly shown that the friction between the tire and pavement is dependent of vehicle speed and the slip ratio at the vehicle maneuvering processes.

In this research, a three-dimensional (3-D) tire-pavement interaction model is developed using FEM to analyze the tire-pavement contact stress distributions at various rolling conditions (free rolling, braking/accelerating, and cornering). In addition, existing friction models for tire-pavement contact are reviewed and the effect of interfacial friction on the tire-pavement contact stress distributions is investigated.

Findings

The developed tire-pavement interaction model shows the potential to predict the tire-pavement contact stress distributions at various rolling and friction conditions. The magnitudes and non-uniformity of contact stresses are affected by the rolling condition as well as the friction at the tire-pavement interface. For example, tire braking/acceleration induces significant longitudinal contact stresses when the tire slides at high slip ratios. The peak contact stresses at tire cornering shift toward to the one side of the contact patch and increases as the slip angle increases. It is reasonable to use the constant friction model when predicting the tire-pavement contact stresses at the free rolling condition or at the

cornering condition with small slip angles. However, it is important to use the sliding-velocity-dependent friction model when predicting the friction force at tire braking. The model results presented in this study provide valuable insights into understanding the realistic tire-pavement interaction for analyzing pavement responses and predicting vehicle stopping distance.

Recommendations

The authors have the following recommendations for the future study:

- Only one specific tire with one type of tread pattern was simulated in this study. It is recommended that various tire types including wide-base tires with different tread patterns should be considered in future studies.
- This study considered pavement as a smooth flat surface and tire deformation is much larger than the pavement deformation. However, deformable road surfaces should be considered in the future study when the tire is loaded on soft terrain, such as snow or soil.

Contacts

For more information:

Imad L. Al-Qadi
University; University of Illinois at Urbana-Champaign
Address: 205 N. Mathews Ave., Urbana, IL, 61801
Phone Number: 217-2650427
Fax Number: 217-8930601
Email Address: alqadi@illinois.edu
Web Address: <http://cee.illinois.edu/node/56>

NEXTRANS Center
Purdue University - Discovery Park
2700 Kent B-100
West Lafayette, IN 47906

nextrans@purdue.edu
(765) 496-9729
(765) 807-3123 Fax

www.purdue.edu/dp/nextrans

ACKNOWLEDGMENTS

The authors acknowledge the assistance and feedback from the members of the study advisory committee. The cost sharing provided by the Illinois Center for Transportation is greatly appreciated.

TABLE OF CONTENTS

	Page
LIST OF FIGURES	iii
CHAPTER 1. INTRODUCTION	1
1.1 Background and Motivation	1
1.2 Study Objectives and Scope	2
1.3 Organization of the Report	2
CHAPTER 2. ISSUES RELATED TO ROLLING TIRE – PAVEMENT CONTACT	4
2.1 Background on Tire Models	4
2.2 Rolling Tire-Pavement Contact Problem.....	6
2.3 Friction at Tire-Pavement Interface.....	9
CHAPTER 3. TIRE-PAVEMENT INTERACTION ANALYSIS.....	14
3.1 Simulation of Tire-Pavement Interaction	14
3.2 Tire-Pavement Contact Stresses at Various Rolling Conditions	18
3.3 Effect of Friction on Tire-Pavement Interaction.....	26
CHAPTER 4. CONCLUSIONS AND RECOMMENDATIONS.....	33
4.1 Conclusions.....	33
4.2 Recommendations.....	34

LIST OF FIGURES

Figure	Page
Figure 2.1 Schematic illustration of a radial-ply tire (after Michelin website on July 27, 2010)	5
Figure 2.2 Contact (a) between two elastic spheres; and (b) between truck tire and pavement under heavy load	7
Figure 3.1 Meshes of Tire Components.....	15
Figure 3.2 Relationship between longitudinal reaction force and angular velocity for a specific transport velocity (10km/h)	19
Figure 3.3 Predicted (a) vertical, (b) transverse, and (c) longitudinal tire-pavement contact stresses at the free rolling condition	20
Figure 3.4 Predicted (a) vertical, (b) transverse, and (c) longitudinal tire-pavement contact stresses at the full braking condition	22
Figure 3.5 Predicted (a) vertical, (b) transverse, and (c) longitudinal tire-pavement contact stresses at the cornering condition.....	24
Figure 3.6 Predicted (a) vertical and (b) transverse contact stress with different slip angles at the cornering condition	25
Figure 3.7 Sliding-velocity-dependent friction models	28
Figure 3.8 Illustrations of the (a) friction force at braking and (b) side force at cornering	30

Figure 3.9 Friction force due to tire braking using different friction models 31

Figure 3.10 Cornering force using different friction models 32

CHAPTER 1. INTRODUCTION

1.1 Background and Motivation

The tire-pavement interfacial contact stresses may cause a complex stress-state near the pavement surface and increase the potential for pavement damages, such as top-down cracking, “near-surface” cracking, and instable rutting in the upper HMA layer (Roque et al. 2001; Al-Qadi and Yoo, 2007; Wang and Al-Qadi, 2009). Hence, accurate modeling of the tire-pavement contact behavior (i.e., distribution of contact tractions at the interface) plays a crucial role in the prediction of near-surface pavement responses.

Several challenges, such as large deformation, transient contact conditions, and intricate structure of the tire, exist when modeling the tire-pavement interaction via a two-solid contact mechanics approach. Thus, it is difficult to solve the tire-pavement contact problem analytically. Hence, numerical methods are necessary and the use of finite element method (FEM) is usually an appropriate choice. This method can address many important aspects of the tire-pavement interaction, such as the composite tire structure (rubber and reinforcement), the nonlinear behavior of tire and pavement material, complex boundary conditions, and temperature effects.

The tire-pavement contact is essentially a rolling contact problem. Many aspects, such as the transient contact with nonlinear frictional properties at the tire-pavement interface, make the rolling contact problem more difficult than it may appear at first glance. The nonlinear frictional contact could introduce numerical difficulties into the FEM solution because the contact area and distribution of the contact tractions are not known beforehand (Stanciulescu and Laursen, 2006). Therefore, it is appealing to formulate and implement high-fidelity finite element (FE) models capable of accurately simulating the tire-pavement contact behavior.

The analysis of tire-pavement contacts requires not only the understanding of the material properties of the tire; but also the knowledge of the vehicle operation and pavement surface condition. It is expected that the development of tangential contact stress is related to the frictional behavior of the contact surfaces. The formation of slipping/adhesion zones in the contact area would change depending on the allowed maximum friction force. However, obtaining an accurate description of the frictional relationship is difficult when modeling the tire-pavement interaction. The friction between the tire and the pavement is a complex phenomenon depending on many factors, such as viscoelastic properties of rubber, pavement texture, temperature, vehicle speed, slip ratio, and normal pressure. Field measurements have clearly shown that the friction between the tire and pavement is dependent on the vehicle speed and on the slip ratio during the vehicle maneuvering processes, such as braking, accelerating, or cornering (Henry, 2000). Therefore, an appropriate friction model is needed to accurately capture the realistic interaction between the tire and pavement at various tire rolling conditions.

1.2 Study Objectives and Scope

This research has two main objectives:

1. Develop a tire-pavement interaction model using the FEM and analyze the tire-pavement contact stress distributions at various rolling conditions (free rolling, braking/accelerating, and cornering).

2. Investigate the effect of interfacial friction on the tire-pavement contact stress distributions at various rolling conditions. Existing friction models for tire-pavement contact will be reviewed, and the appropriate model will be used in the analysis.

1.3 Organization of the Report

This report is divided into four chapters. Chapter 1 introduces the research background and objective. Chapter 2 reviews the issues related to the tire-pavement contact modeling from existing literature. The developed tire-pavement interaction model

using ABAQUS and the analysis results are presented in Chapter 3. The investigators' conclusions and recommendations are presented in Chapter 4.

CHAPTER 2. ISSUES RELATED TO ROLLING TIRE – PAVEMENT CONTACT

2.1 *Background on Tire Models*

The two main types of tires are bias-ply and radial-ply. The radial-ply tire has become more popular because it causes less rolling resistance and heat generation compared to the bias-ply tire. Figure 2.1 shows the typical structure of a radial-ply tire. The radial-ply tire has one or more layers of radial plies in the rubber carcass with a crown angle of 90° . The crown angle is defined as the angle between the ply and the circumferential line of the tire. The radial plies are anchored around the beads that are located in the inner edge of the sidewall and serve as the “boundary” for the carcass to secure the tire casing on the rim. In addition, several layers of steel belts are laid under the tread rubber at a low crown angle. The radial plies and belt layers enhance the rigidity of the tire and stabilize it in the radial and lateral directions. The tread layer of the tire is usually patterned with longitudinal or transverse grooves and serves as a wear-resistance layer that provides sufficient frictional contact with the pavement and minimizes hydroplaning through good drainage of water in wet conditions (Wong, 2002).

The tire industry has developed simplified physical models to predict tire performance. These models include the classical spring-damper model, the tire-ring model, and the membrane and shell model (Knothe et al. 2001). These models are usually unsuitable for quantitative prediction of tire-pavement contact stresses. The FE method is used because it can simulate the complex tire structure (tread, sidewall, radial ply, belt, bead, etc.) and consider representative material properties of each tire component. General-purpose FE commercial codes developed in the mid 1990s, such as

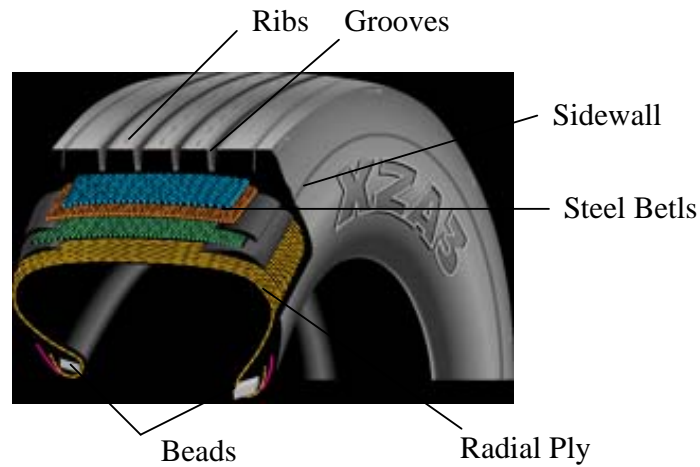


Figure 2.1 Schematic illustration of a radial-ply tire (after Michelin website on July 27, 2010)

ABAQUS, ANSYS, ADINA, etc., provide several tools to simulate 3-D tire behavior with rolling contact. A survey of existing literature reveals many published works on FE simulations of tires. The complexity of tire models varies; it depends on the features built into the model, including the types of FE formulation (Lagrangian, Eulerian, or Arbitrary Lagrangian Eulerian), material models (linear elastic, hyperelastic, or viscoelastic), type of analysis (transient or steady state), and treatment of coupling (isothermal, non-isothermal, or thermo-mechanical). Such tire models allow one to analyze the energy loss (rolling resistance), tire-terrain interaction, steady-state or transient responses, vibration and noise, and tire failure and stability.

From a pavement perspective, the contact stresses developed at the tire-pavement surface are important because they determine the stresses caused in the pavement structure. Tielking and Robert (1987) developed a FE model of a bias-ply tire to analyze the effect of inflation pressure and load on tire-pavement contact stresses. The pavement was modeled as a rigid flat surface and the tire was modeled as an assembly of axisymmetric shell elements positioned along the carcass mid-ply surface. Zhang (2001) built a truck tire model using ANSYS and analyzed the inter-ply shear stresses between the belt and carcass layers as a function of normal loads and pressures. Shoop (2001) simulated the coupled tire-terrain interaction and analyzed the plastic deformation of soft

soil/snow using an Arbitrary Lagrangian Eulerian adaptive mesh formulation. He suggested that the assumption of a rigid tire might be suitable for soft terrain analysis. Roque et al. (2000) used a simple strip model to simulate the cross section of a tire and concluded that the measurement of contact stresses using devices with rigid foundation was suitable for the prediction of pavement responses. Meng (2002) modeled a low profile radial smooth tire on rigid pavement surface using ABAQUS, and analyzed the vertical contact stress distributions under various tire loading conditions. Ghoreishy et al. (2007) developed a 3-D FE model for a 155/65R13 steel-belted tire and carried out a series of parametric analyses. They found that the belt angle was the most important constructional variable for tire behavior and the change of friction coefficient had great influence on the pressure field and relative shear between tire treads and road.

2.2 Rolling Tire-Pavement Contact Problem

Contact mechanics is the study of the stresses and deformations that arise when the surfaces of two solid bodies are brought into contact. The original work on contact mechanics between two frictionless elastic solids was conducted by Hertz (1882). In Hertz contact theory, the localized stresses that develop as two curved surfaces come in contact are dependent on the normal contact force, the radius of curvature of both bodies, and the modulus of elasticity of both bodies. The Hertz contact theory has many practical applications in industry such as tribology and the design of gears and bearing. In the classical Hertz contact theory, the contact radius and pressure between two cylinders can be calculated using Equations 2.1 and 2.2. (Figure 2.2(a)).

$$p = \frac{3P}{2\pi a^2} \sqrt{1 - (r/a)^2} \quad (2.1)$$

$$a = \left(\frac{3PR}{4E^*} \right)^{1/3}, \quad (2.2)$$

where,

P is the applied load; a is the radius of contact area;

p is the pressure at radius distance r ;

R is the relative radius of contact surfaces with $\frac{1}{R} = \frac{1}{R_1} + \frac{1}{R_2}$;

R_1 and R_2 are the radii of the two contact surfaces;

E^* is the contact modulus and $\frac{1}{E^*} = \frac{1}{E_1} + \frac{1}{E_2}$; and

E_1 and E_2 are the elastic moduli of the two objects in contact.

Several differences exist between the assumptions of Hertz contact theory and the real tire-pavement contact, as shown in Figure 2.2(b). These differences include: 1) the tire is pneumatic (hollow) with pressurized inner surface rather than solid; 2) the tire deformation is non-uniform due to the compression of the tire ribs and to the bending of the tire sidewall; 3) the tire is a composite structure that consists of soft rubber and stiff reinforcement; 4) the tire-pavement contact surface is not frictionless and may include inelastic behavior; 5) the contact area is more rectangular than circular and the tire tread is not smooth but has longitudinal/transverse grooves. Therefore, it is difficult to obtain the accurate contact stress distribution at the tire-pavement interface using the classical Hertz contact theory.

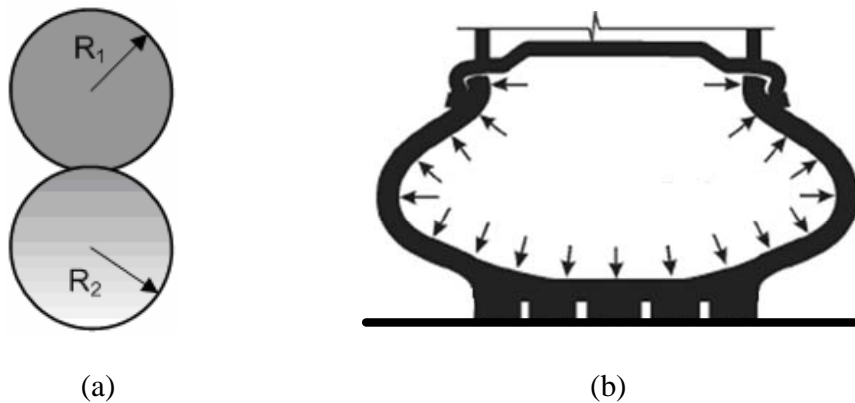


Figure 2.2 Contact (a) between two elastic spheres; and (b) between truck tire and pavement under heavy load

In computational mechanics, two classical descriptions of motion are available: the Lagrangian formulation and the Eulerian formulation. The Eulerian formulation is

widely used in fluid mechanics; the computational mesh is fixed and the continuum moves with respect to the mesh. The Lagrangian formulation is mainly used in solid mechanics; in this description each individual node of the computational mesh follows the associated material particle during the motion. However, it is cumbersome to model rolling contact problem using a traditional Lagrange formulation since the frame of reference is attached to the material. In this reference frame a steady-state tire rolling is viewed as a time-dependent process and each point undergoes a repeated process of deformation. Such analysis is computationally expensive because a transient analysis must be performed for each time step and a refined mesh is required along the entire tire surface (Faria et al. 1992).

An Arbitrary Lagrangian Eulerian (ALE) formulation combines the advantages of the Lagrangian and Eulerian formulations for solving the steady-state tire rolling problem (Hughes et al. 1981; Nackenhorst, 2004). The general idea of ALE is the decomposition of motion into a pure rigid body motion and the superimposed deformation. This kinematic description converts the steady moving contact problem into a pure spatially dependent simulation. Thus, the mesh need be refined only in the contact region and the computational time can be significantly reduced.

Another crucial point in the solution of the rolling contact problem is a sound mathematical description of the contact conditions. Contact problems are nonlinear problems and they are further complicated by the fact that the contact forces and contact patches are not known a priori. A solution to a contact problem must satisfy general basic equations, equilibrium equations and boundary conditions.

The popular approach to solve the contact problem is to impose contact constraint conditions using nonlinear optimization theory. Several approaches are used to enforce non-penetration in the normal direction, amongst which the mostly used are the penalty method, the Lagrange multipliers method or the augmented Lagrangian method (Wriggers, 2002). If there is friction between two contacting surfaces, the tangential forces due to friction and the relative stick-slip behavior needs to be considered. The frequently used constitutive relationship in the tangential direction is the classical Coulomb friction law. This model assumes that the resistance to movement is

proportional to the normal stress at an interface. In this case, the interface may resist movement up to a certain level; then the two contacting surfaces at the interface start to slide relative to each another. If the relative motion occurs, the frictional stress remains constant and the stress magnitude is equal to the normal stress at the interface multiplied by the friction coefficient.

2.3 Friction at Tire-Pavement Interface

The development of the friction force between rubber and a rough hard surface has two effects that are commonly described as the adhesion and hysteretic deformation, respectively. The adhesion component is the result of interface shear and is significant for a clean and smooth surface. The magnitude of the adhesion component is related to the product of the actual contact area and the interface shear strength. The hysteresis component is the result of damping losses and energy dissipation of the rubber excited by the surface asperities (Kummer and Meyer, 1969).

Because the mechanics of friction is very complex as a consequence of many interacting phenomena, the friction behavior between tire and pavement is usually determined experimentally. Pavement friction is defined as the retarding tangential force developed at the tire-pavement interface that resists longitudinal sliding when braking forces are applied to the vehicle tires or sideways sliding when a vehicle steers around a curve. The sliding friction coefficient is computed using Equation 2.3. The type of equipment used for testing tire-pavement friction varies among transportation agencies. Common techniques include the locked wheel tester using a smooth or ribbed tire, fixed slip device, variable slip device, and side force device. Experimental measurements have shown that the friction force at tire-pavement interface is influenced by many factors, including vehicle factors (load, speed, slip ratio, slip angle, camber angle), tire factors (tire type, inflation pressure, tread design, rubber composition), surface conditions (roughness, micro- and macro-texture, dryness and wetness), and environmental factors (temperature and contamination) (Henry, 2000; Hall, et al., 2006).

$$\mu = F_h / F_v , \quad (2.3)$$

where,

μ is the sliding friction coefficient;

F is the tangential friction force at the tire-pavement surface; and

F_v is the vertical load on tire.

A number of friction models have been developed to characterize the tire-pavement friction behavior in vehicle dynamics and stability control. The “Magic Formula” is a well-known empirical model used in vehicle handling simulations, as shown in Equation 2.4 (Pacejka, 2006). The “Magic Formula” can be used for characterizing the relationships between the cornering force and slip angle, between the self-aligning torque and slip angle, or between the friction force and slip ratio. This model has been shown to suitably match experimental data obtained under various testing conditions, although the model parameters do not have physical meanings.

$$F(s) = c_1 \sin(c_2 \arctan(c_3 s - c_4 (c_3 s - \arctan(c_3 s)))) \quad (2.4)$$

where,

$F(s)$ is the friction force due to braking or lateral force or self-aligning torque due to cornering;

c_1 , c_2 , c_3 , and c_4 are model parameters; and

s is the slip ratio or slip angle.

The slip angle is the angle between the actual rolling direction of the tire and the direction towards which it is pointing. The slip ratio is defined as in Equation 2.5. When the tire is free rolling there is no slip, so the slip speed and slip ratio are both zero. When the tire is locked, the slip speed is equal to the vehicle speed and the slip ratio is 100%.

$$s = \frac{v - \omega \cdot r}{v} \cdot 100\% = \frac{v_s}{v} \cdot 100\% \quad (2.5)$$

where,

s is the slip ratio (in percent); v is the vehicle travel speed;

ω is the angular velocity of the tire;

r is the free rolling radius; and

v_s is the slip speed.

Savkoor (1986) found that friction of rubber polymers is closely related to its viscoelastic behavior due to the flexibility of polymer chains. He proposed a formulation that incorporated the effect of the sliding velocity on the friction coefficient, as shown in Equation 2.6. In this equation, the friction coefficient increases with sliding velocity until a maximum value is reached at a certain speed, followed by a decrease of the friction coefficient.

$$\mu_s = \mu_0 + (\mu_m - \mu_0) \exp[-h^2 \log^2(v_s / v_m)] \quad , \quad (2.6)$$

where,

μ_0 is the static friction coefficient;

μ_s is the sliding friction coefficient;

μ_m is the maximum value of μ_s at the slip speed of v_m ;

v_s is the slip speed; and

h is the dimensionless parameter reflecting the width of the speed range in which friction varies significantly.

Dorsch et al. (2002) found that the friction coefficient between rubber tire and road surface is a non-linear function of pressure, sliding velocity, and temperature. The function can be formulated as a power law or as a quadratic formula (Equations 2.7 and 2.8).

$$\mu = c_0 p^{c_1} v_s^{c_2} \quad (2.7)$$

$$\mu = c_0 p + c_1 p^2 + c_2 v_s + c_3 v_s^2 + c_4 p v_s \quad (2.8)$$

where,

μ is the friction coefficient,

c_0 , c_1 , c_2 , c_3 , and c_4 are model parameters,

v_s is the slip speed, and

p is the normal pressure.

Extensive measurements have been conducted to measure the friction between the tire and pavement, and the Penn State model is widely used in the pavement field. It relates the friction to slip speed by testing a fully locked tire on pavement surface, as shown in Equation 2.9. It provides a good estimate of the friction when the locked wheel condition is reached (slip ratio =100%).

$$\mu = \mu_0 e^{-v_s / s_p} \quad (2.9)$$

where,

μ is the friction coefficient at slip speed of v_s ;

μ_0 is the static friction coefficient (at zero speed) that is related to pavement surface micro-texture; and

s_p is the speed number that is highly correlated with pavement surface macro-texture.

The Rado model, known also as the logarithmic friction model, is used to model the friction taking place while a tire proceeds from the free rolling to the locked wheel condition, as shown in Equation 2.10. This model describes the two phases that happen in the braking process. During the first phase, the tire rotation is gradually reduced from free rolling to a locked state. During the second phase, the tire reduces its speed under locked state until a complete stop. In the two phases, the corresponding friction coefficient is first increased to the peak friction at the critical slip ratio and then decreases with the increase of the slip ratio.

$$\mu = \mu_{peak} \cdot e^{-\left[\frac{\ln(v_s / s_{peak})}{C}\right]^2}, \quad (2.10)$$

where,

v_s is the slip speed;

s_{peak} is the slip speed at peak friction;

μ_{peak} is the peak friction coefficient;

C is the shape factor mainly dependent on surface texture.

CHAPTER 3. TIRE-PAVEMENT INTERACTION ANALYSIS

3.1 Simulation of Tire-Pavement Interaction

3.1.1 *Model Descriptions and Assumptions*

Theoretically, a tire model should consider the following: 1) the composite structure (rubber and reinforcement) and the significant anisotropy caused by great differences in stiffness between rubber and reinforcement; 2) the large deformation due to flexibility of tire carcass during contact with the pavement surface; 3) the near-incompressibility and the nonlinearity of rubber material. The tire models commonly used for tire design purposes must accurately predict the deformation of the whole tire and the interaction of internal components (such as sidewall, tread, belts, etc) as well. Because this study is focused on the tire deformation as it relates to the contact region and the resulting contact stress distributions at the tire-pavement interface, simpler models can be employed for higher computational efficiency.

Figure 3.1 shows the mesh of each tire component for the modeled radial ply tire with five straight longitudinal ribs (275/80 R22.5). The tire model comprises one radial ply, two steel belts, and a rubbery carcass. The rim was modeled as a rigid body and in contact with the bead at the end of sidewall. To optimize computation speed and resolution, a finer mesh was chosen around the tread zone, and a coarse mesh was used in the sidewall. To ensure the selected mesh in the contact region (tread zone) was accurate, a mesh convergence analysis was conducted with a series of progressively finer meshes. The predicted contact stress results were compared for each mesh until changes in the numerical results of less than 5% were achieved.

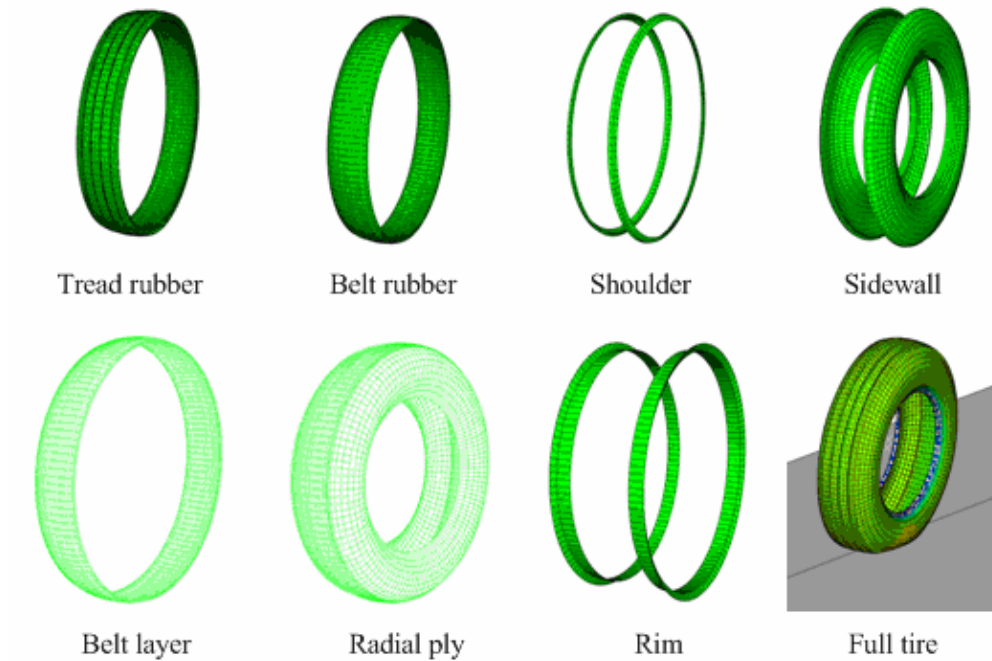


Figure 3.1 Meshes of Tire Components

Rubber is by nature a near-incompressible and hyperelastic material with viscoelasticity. However, the tire industry does not usually make public the exact material properties used in tire design. In this study, the rubber is simulated as a linear elastic material with Poisson's ratio close to 0.5. Different parts of rubber elements (sidewall, shoulder, belt rubber, and tread) are modeled using variable elastic stiffness. The steel reinforcements (radial ply and belts) are modeled as a linear elastic material with high modulus. The elastic properties of rubber and reinforcement are adjusted to obtain values of deflections similar to the experimental measurements. The final selected elastic material properties of each tire component are shown in Table 3.1. More details about the developed tire mode can be found elsewhere (Wang et al. 2010).

Table 3.1 Material Property of Tire Components

Tire components	Material	Elastic modulus (MPa)	Poisson's ratio	Density (kg/m ³)
Tread	Rubber	4	0.49	1100
Belt rubber	Rubber	12	0.49	1100
Sidewall	Rubber	0.5	0.49	1100
Shoulder	Rubber	8	0.49	1100
Radial ply	Nylon	9000	0.3	1500
Belt	Steel	170000	0.3	5900

3.1.2 Modeling of Tire-Pavement Interaction

The tire-pavement interaction was simulated in three load steps. First, the axisymmetric tire model was loaded with uniform tire inflation pressure at its inner surface. Second, the 3-D tire model was generated and placed in contact with pavement under the applied load. Finally, the tire was rolled on pavement with different angular (spinning) velocities and transport velocities. In this study, the pavement was modeled as a non-deformable flat surface. This assumption is considered reasonable because the tire deformation is much greater than the pavement deflection when wheel load is applied on the tire and transmitted to the pavement surface. The large deformation of the tire was taken into account by using a large-displacement formulation in ABAQUS. The tire rolling process was modeled using steady-state transport analysis in ABAQUS/Standard. This analysis utilizes the implicit dynamic analysis and can consider the effect of tire inertia and the frictional effects at the tire-pavement interface.

In the steady-state transport analysis, the Arbitrary Lagrangian Eulerian (ALE) formulation is used rather than traditional Lagrange or Eulerian formulations. The ALE uses a moving reference frame, in which the rigid body rotation is described in an Eulerian formulation and the deformation is described in a Lagrange formulation

(Hughes et al. 1981; Nackenhorst, 2004). This kinematic description converts the steady-state moving contact problem into a pure spatially dependent simulation. Thus, the mesh needs to be refined only in the contact region.

A crucial point in the simulation of the tire-pavement interaction is the appropriate modeling of tire-pavement contact. The contact between the tire and the pavement surface consists of two components: One normal to the pavement surface and one tangential to the pavement surface. The contact constraints are enforced using the penalty method. The non-penetration in the normal direction is enforced. The Coulomb friction law is used to describe the tangential interaction between two contacting surfaces. The contact status is determined by nonlinear equilibrium (solved through iterative procedures) and governed by the transmission of contact forces (normal and tangential) and the relative separation/sliding between two nodes on the surfaces in contact. There are three possible conditions for the nodes at the interface: stick, slip and separation (Equations 3.1-3.3). In the first two cases, nodes are in contact and both normal and tangential forces are transmitted between contacting surfaces. The maximum tangential force is limited by the frictional resistance determined by the Coulomb's law of friction.

$$\text{Stick condition: } g = 0; p < 0; \text{ and } [\tau_1^2 + \tau_2^2]^{0.5} < \mu \cdot p \quad (3.1)$$

$$\text{Slip condition: } g = 0; p < 0; \text{ and } [\tau_1^2 + \tau_2^2]^{0.5} = \mu \cdot p \quad (3.2)$$

$$\text{Separation condition: } g > 0; p = 0; \text{ and } \tau = 0 \quad (3.3)$$

where,

p is the normal force (compression is negative);

g is the gap between two contact nodes;

τ_1 and τ_2 are tangential forces; and

μ is the friction coefficient.

The accuracy of the developed model is validated through comparisons of the predicted tire-pavement contact stresses at the static loading condition to the experimental measurements provided by the tire manufacturer. Measurements were collected as the tire rolled over the instrumentation at a very low speed (close to static). It is noted that the friction between the tire and instrumentation depends on the geometry and interval of sensors used in the measurements. A friction coefficient of 0.3 is selected through a sensitivity analysis because it provides the best match between the predicted and measured contact stresses. More details about the model validation with experimental measurements can be found in other literature (Wang et al. 2010; Al-Qadi and Wang, 2010).

3.2 Tire-Pavement Contact Stresses at Various Rolling Conditions

Tire-pavement contact stresses are affected by various tire rolling conditions such as acceleration, braking, or free rolling. To simulate various tire rolling conditions, the steady-state transport analysis requires the transport velocity (v) and angular velocity (ω) to be specified separately. Because the focus of this study is the effect of friction on the rolling tire-surface interaction, the load on tire is 17.8kN and the tire inflation pressure is 724kPa for all analyses.

3.2.1 Tire-Pavement Contact Stresses at Free Rolling Condition

At the free rolling condition, no additional driving/braking torque is applied on the tire, and the angular velocity is equal to the transport velocity divided by the free rolling radius. For a specific transport velocity, the angular velocity at the free rolling condition can be found through trials until the state that the longitudinal reaction forces (RF) acting on the tire from the pavement surface become zero, as shown in Figure 3.2

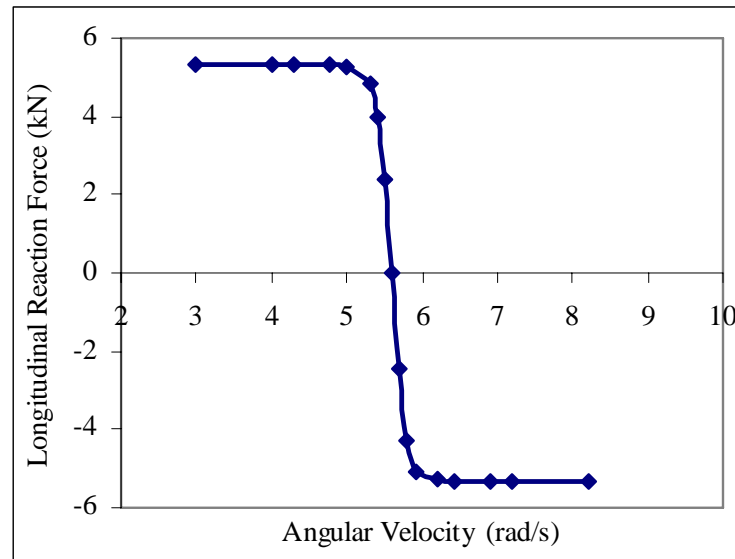
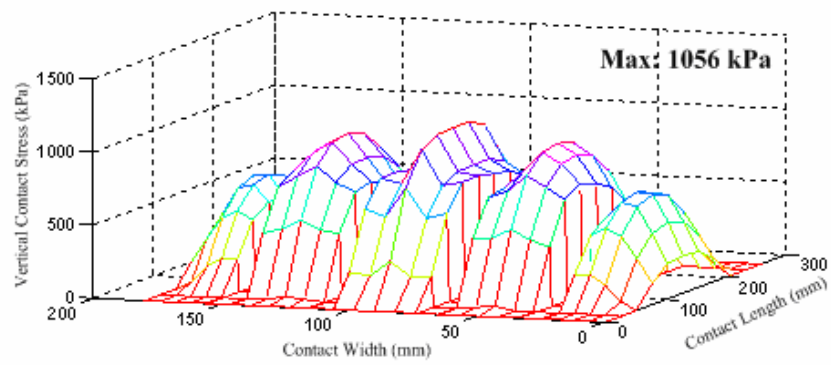
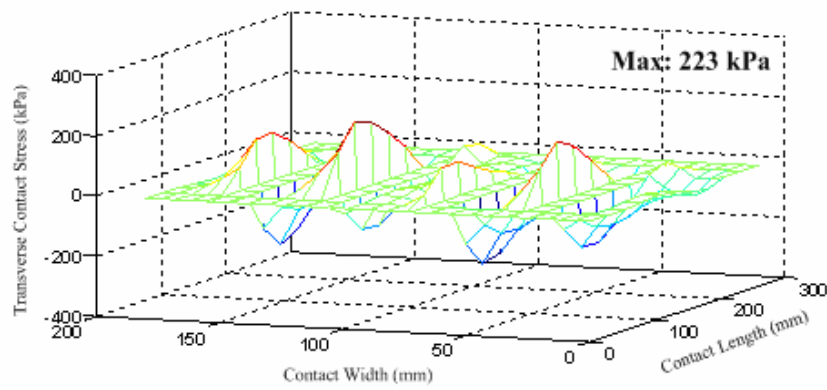


Figure 3.2 Relationship between longitudinal reaction force and angular velocity for a specific transport velocity (10km/h)

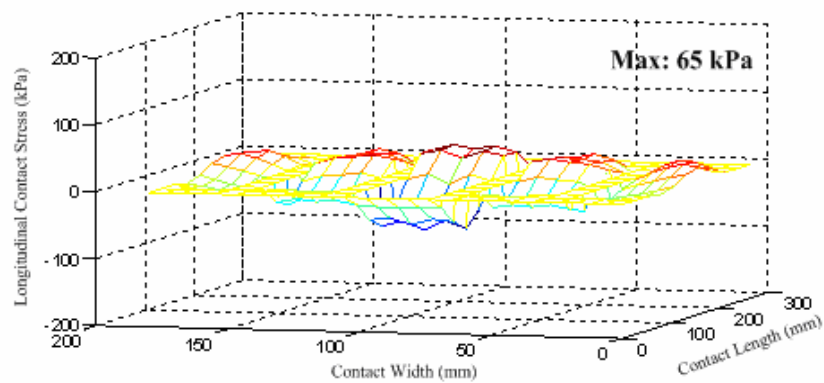
Figures 3.3 (a), (b), and (c) plot the predicted 3-D contact stress fields at the tire-pavement interface at the free rolling condition ($v=10\text{km/h}$, $w=5.6\text{rad/s}$). In the plots, zero values were assigned to the groove areas between adjacent ribs. As the tire is pressed against a flat surface, the tread rubber is compressed in the flattened contact patch and the sidewall of the tire is in tension. The bending stress in the sidewall causes the non-uniform distribution of vertical contact stresses in the contact patch, particularly at the edge of the contact patch. At the same time, the Poisson's effect and the restricted outward movement of each tire rib causes tangential stresses to develop. The plots clearly show that the vertical and transverse contact stresses have a convex shape along the contact length; while the longitudinal contact stresses have a reversed pattern with backward stresses in the front half and forward stresses in the rear half. As expected, the longitudinal contact stresses (frictional forces) are negligible and therefore the tire has low rolling resistance at the free rolling condition. These variations of contact stresses in the contact area are consistent with the reported measurements in the literature (Pottinger, 1992; De Beer et al., 1997; Al-Qadi et al., 2008).



(a)



(b)



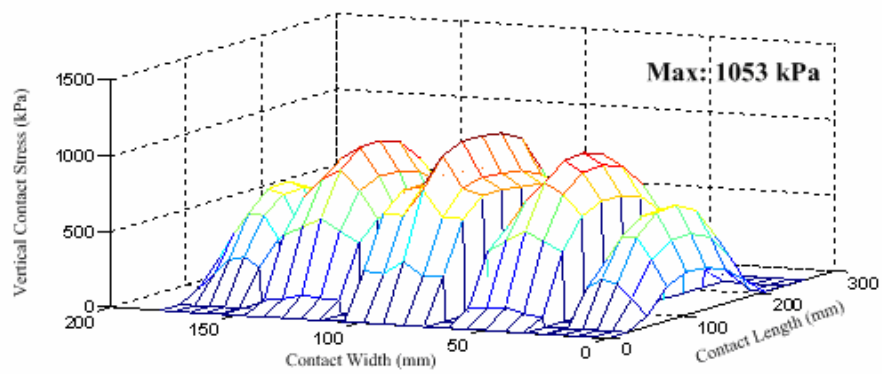
(c)

Figure 3.3 Predicted (a) vertical, (b) transverse, and (c) longitudinal tire-pavement contact stresses at the free rolling condition

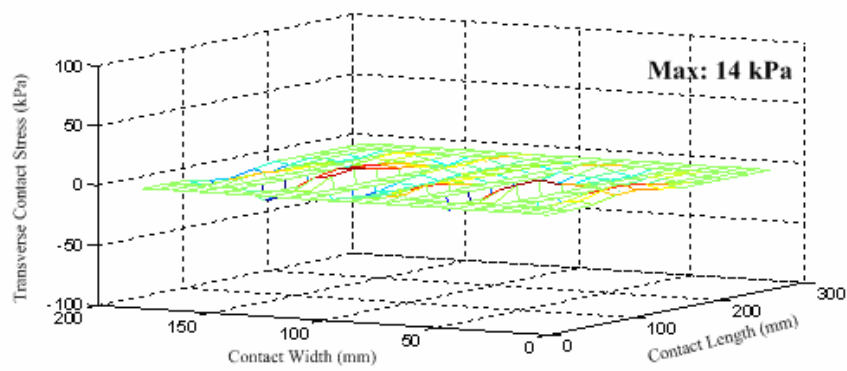
3.2.2 Tire-Pavement Contact Stresses at Braking Condition

During tire braking or acceleration, the angular velocity of the tire is smaller or larger than the angular velocity at the free rolling condition due to the applied braking or driving torque on the tire. Partial braking occurs when the angular velocity of the tire is less than the angular velocity at the free rolling condition such that some of the contact points between the tire and the pavement are sliding. On the other hand, partial acceleration occurs when the angular velocity is greater than the angular velocity at the free rolling condition. Full braking or acceleration occurs at a very slow or fast angular velocity when all the contact points between the tire and the pavement are completely sliding in the backward or forward directions.

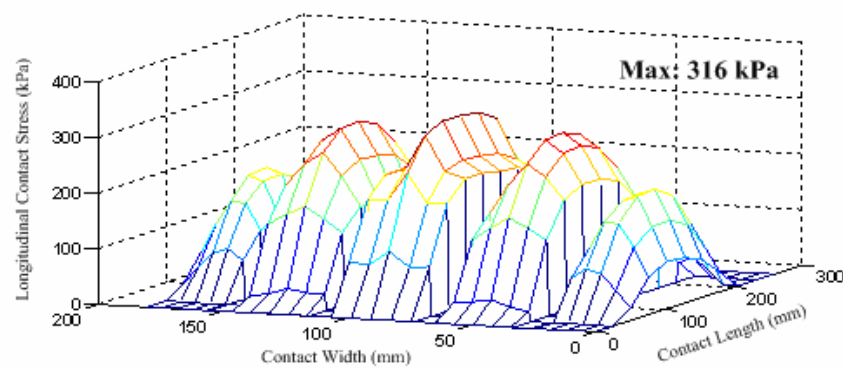
Figures 3.4 (a), (b), and (c) plot the predicted 3-D contact stress fields at the tire-pavement interface at the full braking condition ($v=10\text{km/h}$, $w=3\text{rad/s}$). The effect of weight redistribution between different truck axles due to braking was not considered in the simulation at this point. Compared to the free rolling condition, tire braking causes negligible transverse contact stresses but similar vertical contact stresses and significant longitudinal contact stresses at the tire-pavement interface. Figure 3.4(c) clearly shows that tire braking induces one-directional longitudinal contact stresses when a tire is sliding on a pavement surface, and these stresses are much greater than the longitudinal contact stress at the free rolling condition. The longitudinal contact stresses on a pavement surface during braking and acceleration have similar magnitudes but opposite directions with forward stresses at braking and backward stresses at acceleration. These longitudinal contact stresses may lead to severe pavement deterioration, such as shoving/corrugation and slippage cracking, at pavement intersections or the pavement sections with great longitudinal slopes.



(a)



(b)



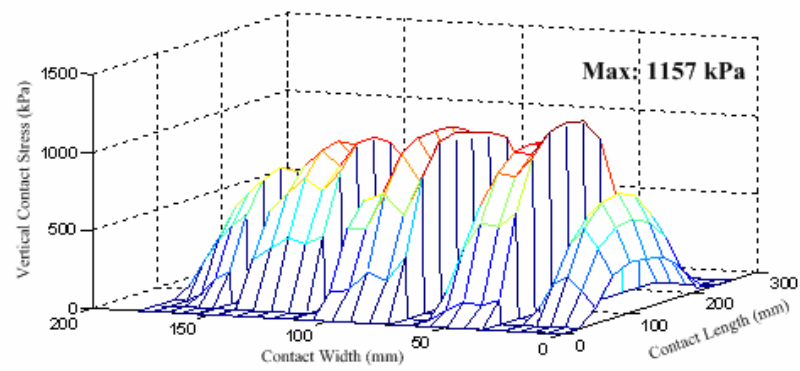
(c)

Figure 3.4 Predicted (a) vertical, (b) transverse, and (c) longitudinal tire-pavement contact stresses at the full braking condition

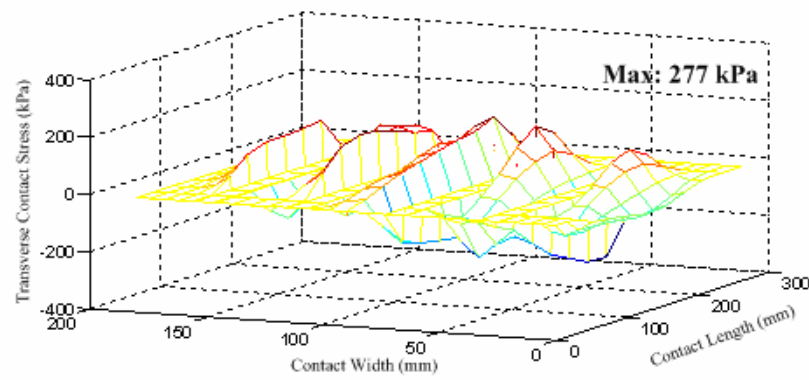
3.2.1 Tire-Pavement Contact Stresses at Cornering Condition

As the tire is cornering, the friction between the tire and road surface restricts the lateral movement of the tire and results in lateral deformation of the tire tread elements within the contact patch while the wheel is steering away from the straight-ahead direction. Therefore, a slip angle is induced between a rolling tire's actual direction of motion and the pointing direction. The slip angle is a measurement of the extent to which the tire contact patch has twisted (steered) in relation to the wheel.

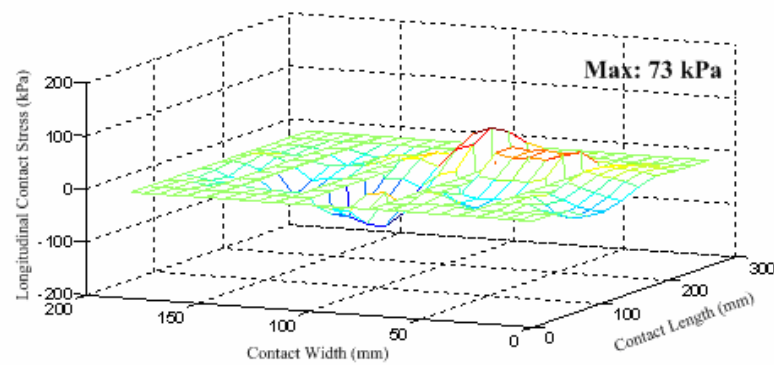
Figures 3.5 (a), (b), and (c) show the predicted 3-D contact stress fields at the tire-pavement interface for cornering condition ($v=10\text{km/h}$, free rolling, slip angle $=1^\circ$). The results show that tire cornering causes concentration of contact stresses shifting toward to the right side of the contact patch, which lies on the inner side of the right turn. This indicates that the right tire shoulder is more strongly compressed to the road surface than the left one during cornering. Hence, the contact stress distribution is no longer symmetric with respect to the center plane and the contact patch is longer on the right side than on the left side. Similar to the free rolling condition, the longitudinal contact stresses at the tire cornering condition are negligible. However, tire cornering causes greater vertical and transverse contact stresses compared to the free rolling condition; the peak contact stresses are concentrated locally at the edge of tire ribs. Localized contact stress concentration at tire cornering could be affected by the tread pattern of the tire (such as tread depth, tread profile, arrangement of ribs and grooves, etc).



(a)



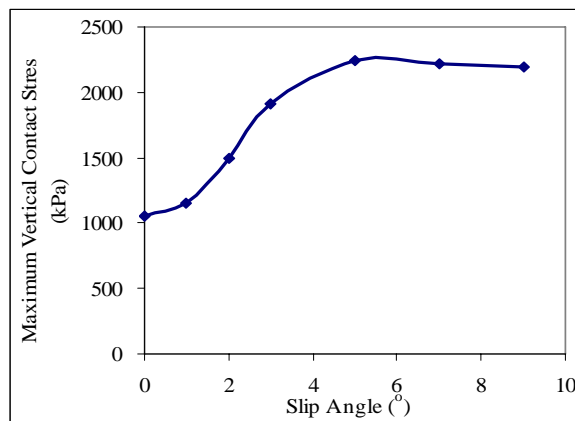
(b)



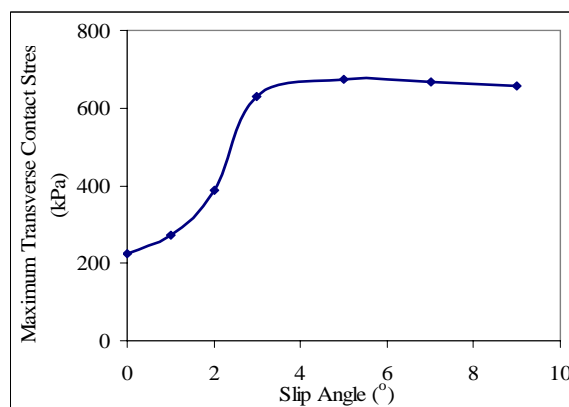
(c)

Figure 3.5 Predicted (a) vertical, (b) transverse, and (c) longitudinal tire-pavement contact stresses at the cornering condition

Figures 3.6 (a) and (b) show the variation of maximum contact stresses with the slip angle at the cornering condition, respectively, for the vertical and transverse contact stresses. As the slip angle increases, the maximum contact stresses increase until the slip angle reaches 5° and then become relatively constant. It was found that the localized stress concentration became more significant as the slip angle increased. The relatively high vertical and transverse contact stresses at tire cornering could explain the accelerated pavement deterioration at the curved road sections where frequent vehicle maneuvering behavior occurs.



(a)



(b)

Figure 3.6 Predicted (a) vertical and (b) transverse contact stress with different slip angles at the cornering condition

3.3 Effect of Friction on Tire-Pavement Interaction

3.3.1 *Effect of Constant Friction Coefficient on Contact Stresses*

Tire-pavement contact stresses are affected by the friction condition at the tire-pavement interface. Table 3.2 summarizes the maximum contact stresses in three directions and the ratio of these maximum contact stresses at various rolling conditions ($v=10\text{km/h}$) when using different friction coefficients. The results show that when the tire is free rolling or full braking, the vertical contact stresses are kept relatively constant as the friction coefficient increases. However, the tangential contact stress increases as the friction coefficient increases, especially for the transverse contact stress at the free rolling condition and the longitudinal contact stresses at the braking condition. This is because the tangential contact stresses develop through shear mechanisms while a tire rolls on a road surface and therefore depend on the friction coupling at the tire-pavement interface. When the tire is cornering, all contact stresses increase as the friction coefficient increases; the increase of vertical and transverse contact stresses is more significant than the increase of longitudinal contact stresses. This is probably because the tire deformation tends to be greater in the one side of the contact patch during cornering as the allowed maximum friction force before sliding increases.

At the free rolling and cornering conditions, the ratios of tangential contact stresses relative to the vertical contact stresses are smaller than the friction coefficients. This indicates that no relative slippage happens between the tire and pavement. However, at full braking, the longitudinal contact stresses are equal to the vertical contact stresses multiplied by the friction coefficient since the tire is essentially sliding on the pavement surface.

TABLE 3.2 Maximum Contact Stresses with Different Friction Coefficients

Rolling conditions	Friction coefficients	Maximum Contact Stresses			Maximum Stress Ratio
		Vertical	Transverse	Longitudinal	
Free rolling	$\mu = 0.3$	1056	223	65	1:0.21:0.06
	$\mu = 0.5$	1051	309	73	1:0.29:0.07
	$\mu = 0.8$	1067	391	81	1:0.37:0.08
Full Braking	$\mu = 0.3$	1053	14	316	1:0.02:0.30
	$\mu = 0.5$	1099	38	549	1:0.03:0.50
	$\mu = 0.8$	1144	73	915	1:0.06:0.80
Cornering (slip angle =1°)	$\mu = 0.3$	1157	277	73	1:0.24:0.06
	$\mu = 0.5$	1302	401	85	1:0.31:0.07
	$\mu = 0.8$	1432	485	95	1:0.34:0.07

3.3.2 Effect of Sliding-Velocity-Dependent Friction Coefficient on Contact Stresses

Experiments have found that, for a rubber tire sliding on pavement surface, the friction between the tire and pavement surface is not constant and is strongly dependent on vehicle speed and slip ratio. In this part, the effect of the sliding-velocity-dependent friction coefficient on the contact behavior at the tire-pavement interface is examined. As shown in Equation 3.4, the friction coefficient is modeled as an exponential function of sliding velocity (Oden and Martins, 1985). This equation defines a smooth transition from a static to a kinetic friction coefficient in terms of an exponential curve.

$$\mu = \mu_k + (\mu_s - \mu_k)e^{-\alpha \cdot s} \quad (3.4)$$

where,

μ_k is the kinetic coefficient at the highest sliding velocity;

μ_s is the static coefficient at the onset of sliding (zero sliding velocity);

α is the user-defined decay coefficient; and

s is the sliding velocity (slip rate).

For the contact between the rubber tire and pavement surface, the static friction coefficient is more related to the surface micro-texture; while the decay coefficient is highly dependent on the surface macro-texture (Henry, 2000). In this study, the static friction coefficient is set to 0.3 to compare contact stresses between the constant friction model and the sliding-velocity-dependent friction model. This static friction coefficient represents the friction condition of the pavement surface with poor micro-texture. Two different values of decay coefficients (0.05 and 0.5) are used to represent the friction characteristics of pavement surface with good and poor macro-texture, respectively (Figure 3.7)

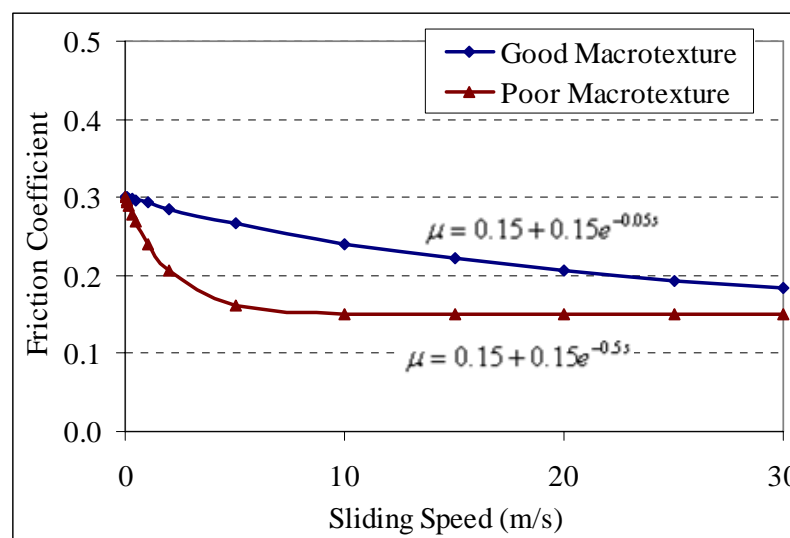


Figure 3.7 Sliding-velocity-dependent friction models

Table 3.3 summarizes the maximum contact stresses in three directions and the ratio of these maximum contact stresses at various rolling conditions when using different friction models ($v = 10\text{km/h}$). The tire-pavement contact stresses at the free rolling condition or at the cornering condition are not affected by the sliding-velocity-dependent friction model because nearly no slip is induced at the tire-pavement interface when the tire is in pure rolling or cornering at small angles. This indicates that it is reasonable to use the constant static friction coefficient when predicting the tire-pavement contact stresses at the free rolling condition or at the cornering condition with small slip angles. However, using the constant friction model may overestimate the peak longitudinal contact stress when the tire is sliding at the full braking condition (the constant friction model cannot simulate the decay of friction coefficient as the slip speed increases).

TABLE 3.3 Maximum Contact Stresses with Different Friction Coefficients

Rolling conditions	Friction Model	Maximum Contact Stresses			Maximum Stress Ratio
		Vertical	Transverse	Longitudinal	
Free rolling	$\mu = 0.3$	1056	223	65	1:0.21:0.06
	$\mu = 0.15 + 0.15e^{-0.05s}$	1056	223	65	1:0.21:0.06
	$\mu = 0.15 + 0.15e^{-0.5s}$	1056	223	65	1:0.21:0.06
Full Braking	$\mu = 0.3$	1053	19	316	1:0.02:0.30
	$\mu = 0.15 + 0.15e^{-0.05s}$	1052	14	306	1:0.01:0.29
	$\mu = 0.15 + 0.15e^{-0.5s}$	1051	10	240	1:0.01:0.23
Cornering with slip angle = 1°	$\mu = 0.3$	1157	277	73	1:0.24:0.06
	$\mu = 0.15 + 0.15e^{-0.05s}$	1157	276	73	1:0.23:0.06
	$\mu = 0.15 + 0.15e^{-0.5s}$	1153	272	73	1:0.23:0.06

3.3.3 Effect of Sliding-Velocity-Dependent Friction Coefficient on Friction Force

The three main functions provided by tires are: a) supporting the vehicle load while cushioning the vehicle against pavement roughness; b) developing longitudinal forces for acceleration and braking; and c) developing lateral forces for cornering (Gillespie, 1993). Figures 3.8 (a) and (b) show the illustrations of the longitudinal friction force during vehicle braking and the side force at cornering, respectively.

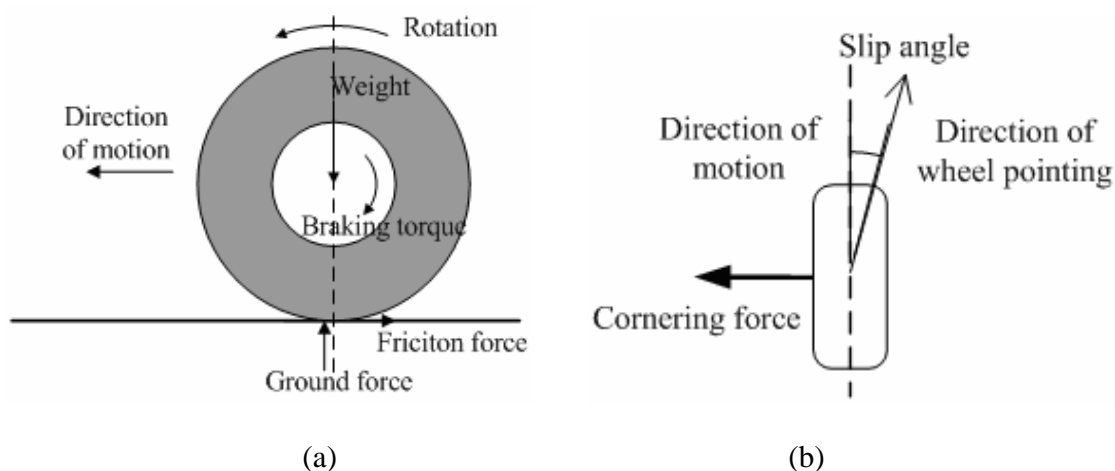


Figure 3.8 Illustrations of the (a) friction force at braking and (b) side force at cornering

Figure 3.9 plots the calculated longitudinal friction force that acts on the tire during braking at different slip ratios. The general trend shows that the friction force reaches its maximum when the slip ratio is around 10% (critical slip ratio). When the slip ratio is lower than the critical slip ratio, the state of contact is partial slip; when the slip ratio is greater than the critical slip ratio, the state of contact is full slip. When the tire is at full slip, the value of the maximum frictional force is equal to the normal force applied on the tire multiplied by the friction coefficient.

It was found that when the tire was at partial slip, the calculated friction forces are approximately the same when using the constant and the sliding-velocity-dependent friction models. However, different trends were observed as the tire was at full slip. For the constant friction coefficient model, the friction force remains constant as the slip ratio

is greater than the critical slip ratio. On the other hand, the friction force decreases as the slip ratio increases when the sliding-velocity-dependent friction model is used. The development trend of friction force using the slide-velocity-dependent model is more consistent with the measured skid resistance during the tire braking process, as indicated in the Rado model. In addition, it was found that using the constant friction model could overestimate the maximum friction force at the critical slip ratio. This is particularly important for the vehicles with an anti-lock braking system (ABS) because the brakes are controlled on and off repeatedly such that the friction force is held near the peak.

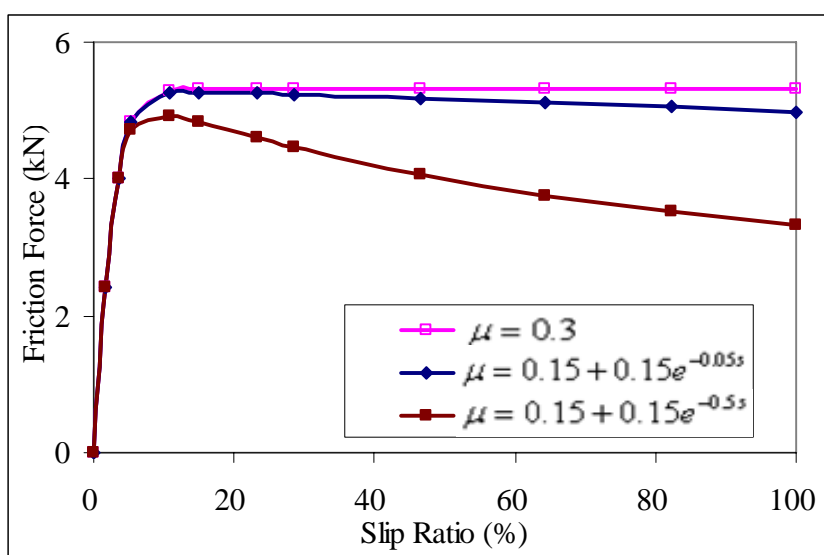


Figure 3.9 Friction force due to tire braking using different friction models

Figure 3.10 shows the cornering forces that act on the tire during cornering at various slip angles. The cornering force (side friction force) is induced on the tire due to the tread slip at lateral direction when the vehicle is steering, which is parallel to the road surface and perpendicular to the wheel's moving direction. The results show that the cornering force increases approximately linearly for the first few degrees of slip angle, and then increases non-linearly to its peak value at the slip angle of around 5° and then stays relatively constant. The relationship between the cornering forces and the slip angles strongly affects the directional control and stability of the vehicle. The

development trend of the cornering force is consistent with the experimental results in the literature (Wong, 2002).

At low slip angles there is little to no slip in the contact area, thus the cornering force is not affected by the friction model. As the tire reaches higher slip angles, the slip occurs in the contact area where the lateral force approaches the available friction force. After the slip occurs, the global lateral force is dominated by the maximum friction force. Thus, the predicted cornering forces at high slip angles using the sliding-velocity-dependent friction model are slightly smaller than those predicted using the constant friction model.

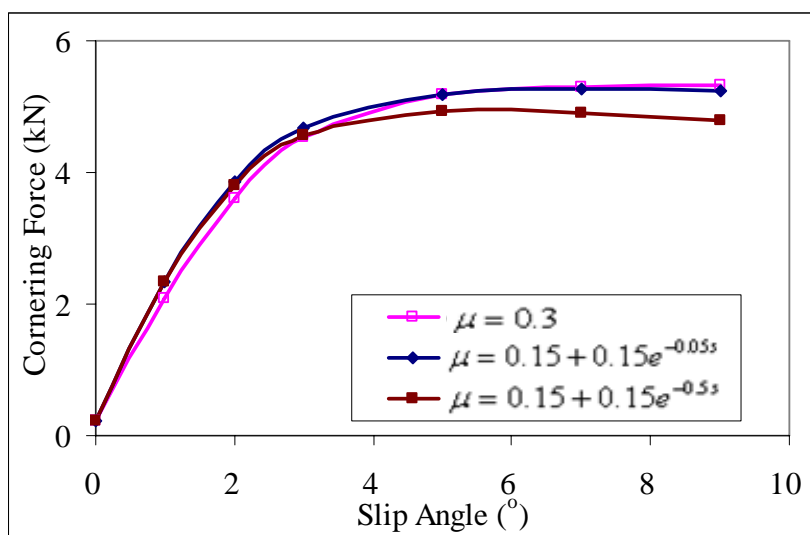


Figure 3.10 Cornering force using different friction models

CHAPTER 4. CONCLUSIONS AND RECOMMENDATIONS

4.1 *Conclusions*

The developed tire-pavement interaction model shows the potential to predict the tire-pavement contact stress distributions at various rolling conditions. The magnitudes and non-uniformity of contact stresses are affected by the rolling condition and as well as the friction at the tire-pavement interface. The following conclusions can be drawn from the analysis:

- 1) A tire-pavement interaction model was developed using the FEM that allows the analysis of tire-pavement contact stress distributions at various rolling conditions (free rolling, braking/accelerating, and cornering).
- 2) At the free rolling condition, three contact stress components are induced at the tire-pavement interface: vertical, transverse, and longitudinal. The maximum stress ratios of the three components are around 1:0.2~0.4:0.1.
- 3) Compared to the free rolling condition, tire braking/acceleration causes reduction in transverse contact stresses but similar vertical contact stresses and significant increase in longitudinal contact stresses at the tire-pavement interface. At the cornering condition, both the vertical and transverse contact stresses are greater than those at the free rolling condition. The peak contact stresses at the cornering condition shift toward to one side of the contact patch (the direction of steering) and increase as the slip angle increases.
- 4) At the free rolling and the braking/accelerating conditions, the tangential contact stresses increase as the friction coefficient increases. At the cornering

condition, both the vertical and tangential contact stresses increase as the friction coefficient increases. This indicates that the proper friction coefficient is important for the accurate prediction of tire-pavement contact stresses.

- 5) It is reasonable to use the constant friction model when predicting the tire-pavement contact stresses at the free rolling condition or at the cornering condition with small slip angles. However, it is important to use the sliding-velocity-dependent friction model when predicting the friction force at tire braking. The constant friction model cannot simulate the decay of friction coefficient as the slip speed increases and thus will overestimate the values of friction force.

4.2 Recommendations

The authors have the following recommendations for the future study:

- 1) Only one specific tire with one type of tread pattern was simulated in this study. It is recommended that various tire types including wide-base tires with different tread patterns should be considered in future studies.
- 2) This study considered pavement as a smooth flat surface and tire deformation is much larger than the pavement deformation. However, deformable road surfaces should be considered in the future study when the tire is loaded on soft terrain, such as snow or soil.

REFERENCES

ABAQUS, (2007), ABAQUS Analysis User's Manual, Version 6.7, Habbit, Karlsson & Sorenson, Inc, Pawtucket, RI

Al-Qadi, I.L., H. Wang, P.J. Yoo, and S.H. Dessouky, (2008), Dynamic Analysis and In-Situ Validation of Perpetual Pavement Response to Vehicular Loading, Transportation Research Record, No. 2087, TRB, Washington, D.C., pp. 29-39

Al-Qadi, I.L. and H. Wang, (2010), Prediction of Tire-Pavement Contact Stresses and Analysis of Pavement Responses: A Decoupled Approach, Accepted for publication in the Journal of the Association of Asphalt Paving Technologists, 2010

Al-Qadi, I.L. and P.J. Yoo, (2007), Effect of Surface Tangential Contact Stress on Flexible Pavement Response, Journal of the Association of Asphalt Pavement Technologist, Vol. 76, pp. 663-692

Andresen, A., J.C. Wambold, (1999), Friction Fundamentals, Concepts and Methodology, Prepared for Transportation Development Centre Transport Canada

De Beer, M., C. Fisher and F.J. Jooste, (1997), Determination of Pneumatic Tire Pavement Interface Contact Stresses Under Moving Loads and Some Effects on Pavements with Thin Asphalt Surfacing Layers, Proceedings of 8th International Conference on Asphalt Pavements (Volume I), Seattle, Washington, pp. 179-227.

Dorsch, V., A. Becker, and L. Vossen, (2002), Enhanced Rubber Friction Model for Finite Element Simulations of Rolling Tires, *Plastics Rubbers and Composites*, 31(10), pp. 458-464

Gillespie, T.D., (1992) Fundamentals of Vehicle Dynamics, Society of Automotive Engineers (SAE), Warrendale, Pennsylvania

Ghoreishy, M.H.R., M. Malekzadeh, H. Rahimi, (2007), A Parametric Study on the Steady State Rolling Behavior of a Steel-Belted Radial Tire, *Iranian Polymer Journal*, 16, pp. 539-548.

Hall, J.W., L.T. Glover, K.L. Smith, L.D. Evans, J.C. Wambold, T.J. Yager, and Z. Rado, (2006), Guide for Pavement Friction. Project No. 1-43, Final Guide, National Cooperative Highway Research Program, TRB, Washington D.C.

Henry, J. J., (2000), Evaluation of Pavement Friction Characteristics, NCHRP Synthesis 291, TRB, National Research Council, Washington, D.C.

Hughes, T.J.R., W.K. Liu, and T.K. Zimmermann, (1981), Lagrangian–Eulerian Finite Element Formulation for Incompressible Viscous Flows, *Computer Methods in Applied Mechanics and Engineering*, 29, pp. 329–349.

Knothe, K., R. Wille, B.W. Zastra, (2001), Advanced Contact Mechanics – Road and Rail, *Vehicle System Dynamics*, Vol. 35, Numbers 4-5, pp. 361-407.

Meng, L., (2002), Truck Tire/Pavement Interaction Analysis by the Finite Element Method, Ph.D. Dissertation, Michigan State University, USA

Nackenhorst, U., (2004), The ALE-Formulation of Bodies in Rolling Contact - Theoretical Foundations and Finite Element Approach, *Computation Methods in Applied Mechanics and Engineering*, Vol. 193, pp 4299–4322.

Oden, J.T. and J.A.C. Martins, (1985), Models and Computational Methods for Dynamic Friction Phenomena, *Computer Methods in Applied Mechanics and Engineering*, Vol. 52, Issues 1-3, pp. 527-634

Pacejka, H.B., (2006), *Tire and Vehicle Dynamics*, Butterworth-Heinemann, 2nd edition

Pottinger, M.G., (1992), Three-Dimensional Contact Patch Stress Field of Solid and Pneumatic Tires, *Tire Science and Technology*, Vol. 20, No. 1, pp. 3-32

Roque, R., L. Myers, and B. Ruth, (2000), Evaluating Measured Tire Contact Stresses to Predict Pavement Response and Performance, Transportation Research Record, No. 1716, TRB, Washington, D.C., pp. 73-81.

Savkoor, A.R., (1986), Mechanics of Sliding Friction of Elastomers, Wear, 113, PP. 37–60

Shoop, S.A., (2001), Finite Element Modeling of Tire-Terrain Interaction, Ph.D. Dissertation, University of Michigan, USA

Tielking, J.T., and M.A. Abraham, (1994), Measurement of Truck Tire Footprint Pressures, Transportation Research Record, No. 1435, TRB, Washington, D.C., pp. 92–99.

Tielking, J.T. and F.L. Roberts, (1987), Tire Contact Pressure and Its Effect on Pavement Strain, Journal of Transportation Engineering, Vol. 113, No. 1, ASCE, pp. 56-71.

Wang, H. and I.L. Al-Qadi, (2009), Combined Effect of Moving Wheel Loading and Three-Dimensional Contact Stresses on Perpetual Pavement Responses, Transportation Research Record, No. 2095, TRB, Washington, D.C., pp. 53-61.

Wang, H., I.L. Al-Qadi, and I. Stanciulescu, (2010), Simulation of Tire-Pavement Interaction for Predicting Contact Stress at Static and Various Rolling Conditions, Submitted for publication in International Journal of Pavement Engineering.

Wong, J.Y., (1993), Theory of Ground Vehicles, John Wiley & Sons, Inc., New York, NY

Wriggers, P., (2002), Computational Contact Mechanics, John Wiley & Sons Ltd

Zhang, X., (2001), Nonlinear Finite Element Modeling and Incremental Analysis of A Composite Truck Tire Structure, Ph.D. Dissertation, Concordia University, Canada, 2001